Applied Catalysis B: Environmental 199 (2016) 134–141

Contents lists available at ScienceDirect

Applied Catalysis B: Environmental

journal homepage: www.elsevier.com/locate/apcatb

Cobaloxime coenzyme catalyzing artificial photosynthesis for hydrogen generation over CdS nanocrystals

Fujun Niu, Shaohua Shen*, Ning Zhang, Jie Chen, Liejin Guo

International Research Centre for Renewable Energy, State Key Laboratory of Multiphase Flow in Power Engineering, Xi'an Jiaotong University, Shaanxi 710049, China

ARTICLE INFO

Article history:
Received 22 April 2016
Received in revised form 8 June 2016
Accepted 9 June 2016
Available online 11 June 2016

Keywords:
Artificial photosynthesis
Cobaloxime coenzyme
Hydrogen generation

ABSTRACT

Inspired by the natural photosynthesis, artificial photosynthesis (AP) systems comprised of light harvesters and redox catalysts have been widely investigated for photocatalytic H_2 generation. Here we report an artificial photosynthesis system composed of CdS nanocrystals as photosensitizer, cobaloxime coenzyme ($Co(dmgBF_2)_2(H_2O)_2$, **Co**) as catalyst, and lactic acid (LA) as electron donor for H_2 generation in a fully aqueous solution. This CdS/**Co**/LA system exhibits exceptional high photocatalytic activity under visible light, with initial H_2 generation rate increased by 4000% compared to CdS/LA, which is even 700% as high as that of CdS/Pt/LA. The excellent photocatalytic performance of CdS/**Co**/LA should be attributed to the efficient electron transfer from CdS to **Co**, leading to the reduced charge recombination, as well as the positively shifted Fermi level of CdS, decreasing the overpotential for H_2 generation. Moreover, the electron-coupling-electron-coupling (ECEC) mechanism, involving with the reduction of **Co** coenzyme followed by protonation and then reduction again, was supposed to produce the **Co**(II)-H intermediate active for catalyzing H_2 evolution from aqueous solution.

1. Introduction

As inspired by photosynthesis in nature, artificial photosynthesis (AP) for converting sunlight to chemical fuels by water splitting has emerged as a promising approach to deal with the energy and environment issues [1–7]. As light absorbers desirable for AP, semiconductors are more competitive and promising for their excellent photostability, broad spectral response, and long lifetime of excited states in photocatalysis for H_2 generation, when compared with the organic or organometallic molecules [8–13]. Among these semiconductors developed for photocatalytic H_2 production, CdS has captured intensive attentions, owing to the suitable bandgap and excellent solar light response property [14,15]; and thus extremely high photocatalytic activity for solar H_2 generation has been achieved over CdS [15,16]. However, in these CdS photocatalytic systems, particulate noble metals (e.g., Pt, Pd, Au) as cocatalysts are indispensable to maintain the high activity and stability of CdS for H_2 generation [17,18]. Moreover, these noble-metal atoms aggregated particulate cocatalysts are of relatively low atom utilizations, poorly designable structures, and lacking in adjustment of physical and chemical properties. In contrast, bioinspired molecules made of earth-abundant elements (e.g., Fe, Co, Ni) as cocatalysts are of great potential and practical significance for AP systems for photocatalytic H_2 production, because of their low cost, high atom utilization, designable structures, and adjustable physicochemical and redox properties [9].

In the past decades, cobaloxime coenzymes have been widely studied and used as molecular catalysts in electrocatalytic [19–21] and photocatalytic [22,23] systems for H_2 production due to their low reduction overpotential, oxygen-tolerant property, earth-abundant resources, and relatively high activity. For example, $[Co^{III}(dmgH)_2(py)Cl]$ and $[Co(dmgH)(dmgH_2)]_2L_2$ could efficiently catalyze H_2 production from H_2O/CH_3CN solution using organic dyes as light harvester, giving the turnover number (TON vs. cobaloxime coenzymes) as high as 50 after 24 h and 1134 after 2 h irradiation, respectively [24–28]. However, these cobaloxime molecules always need to be dissolved in organic solvents like CH_3CN for efficient H_2 evolution, which greatly limits their application in solar H_2 generation via water splitting. Sun and co-workers used a water-soluble cobaloxime coenzyme $Co(dmgBF_2)_2(H_2O)_2$ (**Co**) to catalyze H_2 generation using organic dyes as the light harvester, giving TON of 2 based on **Co** in 6 min from H_2O/CH_3CN

* Corresponding author.
E-mail address: shshen_xjtu@mail.xjtu.edu.cn (S. Shen).

http://dx.doi.org/10.1016/j.apcatb.2016.06.029
0926-3373/

solution [29] and TON of 21 in 5 h from aqueous solution [30], respectively. It is generally accepted that hybrid systems using semiconductors rather than organic dyes as light harvesters are always more stable and robust for photocatalytic H_2 generation than those organic-photosensitizer AP systems [8,9,31]. For example, Huang et al. constructed a hybrid AP system using a cobalt(III) bisglyoximate molecule as the catalyst and CdSe/ZnS core/shell quantum dots as the light harvester for photocatalytic H_2 evolution from toluene containing hydrochloride acid as proton provider and triethanolamine (TEOA) as sacrificial electron donor, giving a high TON of 150 based on the cobaloxime catalyst after 10 h irradiation [22]. However, there is still rare report on noble-metal-free hybrid AP systems using $Co(dmgBF_2)_2(H_2O)_2$ (**Co**) as the catalyst and inorganic semiconductors as the light harvesters for photocatalytic H_2 generation in fully aqueous solution.

Herein, an inexpensive hybrid AP system was designed for H_2 generation under visible light irradiation, which was composed of CdS nanocrystals as the light harvester, **Co** coenzyme as the redox catalyst and lactic acid (LA) as the sacrificial electron donor in aqueous solution. This CdS/**Co**/LA system exhibited impressive high H_2 evolution activity from water rather than organic solvents, which is 40 times higher than that of CdS/LA system and even 7 times higher than that of CdS/Pt/LA system. The excellent photocatalytic performance of the CdS/**Co**/LA system should be attributed to the efficient electron transfer from CdS to **Co**, leading to promoted charge separation and reduced charge recombination, as well as the positively shifted Fermi level of CdS induced by **Co**, lowering the energy barrier for H_2 generation at the CdS/electrolyte interface. By monitoring the electrochemical and photocatalytic properties of the CdS/**Co**/LA system, the electron-coupling-electron-coupling (ECEC) mechanism, involving with the reduction of **Co** coenzyme followed by protonation and then reduction again, as supposed to produce the **Co**(II)-H intermediate active for catalyzing H_2 evolution. The present study made a deep insight into the catalysis mechanisms at the semiconductor/electrolyte interface, including Fermi level engineered interface charge transfer and catalyst-driven surface water reduction processes, and could provide some referable principles to guide the design of highly efficient hybrid AP system for H_2 generation from fully aqueous solution.

2. Experimental

2.1. Preparation of CdS nanocrystals

All the chemicals are of analytical grade and used as received except noted. CdS was synthesized by a solvothermal method [32]. Typically, 0.1484 g of $Cd(Ac)_2{\cdot}H_2O$ was added to 56 mL of dimethylsulfoxide (DMSO) and stirred for 10 min. Then, the solution was transferred into a 70 mL Teflon-lined autoclave and held at 180 °C for 12 h. After cooled to room temperature naturally, the product was collected by centrifugation, washed extensively with acetone and alcohol, and dried at 60 °C for 8 h in a vacuum oven.

2.2. Preparation of the cobalt complex

$Co(dmgBF_2)_2(H_2O)_2$ (**Co**) was synthesized according to the literature [33]. 10 mL of $BF_3{\cdot}Et_2O$, 2.0 g of $Co(Ac)_2{\cdot}4H_2O$ and 1.9 g of dimethylglyoxime (DMSO) were added to 150 mL of ether and stirred at room temperature for 6 h under N_2 atmosphere. The resulting suspension was filtered and dried at room temperature for 6 h in a vacuum oven. A brown solid product was obtained (4.0 g, 9.6 mmol, 60% yield).

2.3. Preparation of CdS, CdS/Pt and CdS/**Co** films

CdS film was prepared by a simple electrophoretic deposition. In a typical deposition process, 50 mg of the as-prepared CdS was added to 30 mL of acetone under stirring and then ultrasonically dispersed for 30 min. Two parallel FTO substrates were soaked vertically into the obtained suspension at a distance of 3 cm for electrophoretic deposition under bias of 10 V for 5 min using an Electrochemical Workstation. Then the as-prepared film was dried at 60 °C for 12 h in a vacuum oven. CdS/Pt film was prepared using a simple sputtering method by coating Pt on the surface of the as-prepared CdS film using JFC-1600 auto fine coater. CdS/**Co** film was fabricated by soaking the prepared CdS film into **Co** aqueous solution for 30 min under stirring. Then the obtained film was washed by water for several times and dried at 50 °C for 12 h in a vacuum oven.

2.4. Characterization of samples

Crystal structure of CdS was examined by a powder X-ray diffractometer (X'Pert PRO MPD, PANalytical, the Netherlands) with (θ/2θ) Bragg–Brentano geometry. The powder X-ray diffraction (PXRD) patterns were collected in the range 2θ = 10–80° (40 kV, 40 mA; Cu Kα radiation, λ = 1.541874 Å; Ni filter; realtime multiple strip (RTMS) detector, X' Celerator). UV–vis diffuse reflectance spectra of the prepared CdS and **Co** were recorded by a Hitachi U-4100 UV–vis-near-IR spectrophotometer employing $BaSO_4$ as reference, and UV–vis diffuse reflectance spectra of the solutions were recorded with the related blank aqueous solution as reference. Brunauer-Emmett-Teller (BET) surface area of CdS was performed at Accelerated Surface Area and Porosimetry Analyzer (ASAP 2020, Micromeritics, USA) after degassing the sample at 120 °C for 3 h and determined from N_2 adsorption-desorption isotherms at 77 K. Photoluminescence (PL) emission spectra were recorded with a PTI QM-4 fluorescence spectrophotometer. CdS was ultrasonically dispersed in ethanol, and then, by dipping and drying process, deposited on copper grids for transmission electron microscopy (TEM) analysis (G2 F30, FEI, USA). The experimental element analysis of **Co** is obtained by elemental analyzer (vaeeio MACRO cube, Elementar, Germany) and X-ray fluorescence spectrum (XRF) (S4 PIONEER, Bruker, USA). Electrospray ionization mass spectrometry (ESI–MS) spectra of **Co** was performed by AXIMA-CFR^{TM} plus MALDI-TOF Mass Spectrometer instrument. Photocurrent measurements were carried out on a potentiostat (273A, Princeton Applied Research Company, USA) in a two-electrode cell system without any bias potential. The as-prepared films and a large area platinum plate were employed as working electrode and counter electrode, respectively.

2.5. Photocatalytic hydrogen production

The photocatalytic hydrogen production experiments were carried out in a gas-closed circulation system with the 257 mL Pyrex glass cell as the photoreactor, which had a flat, round side-window for external light incidence. A 300 W Xe arc lamp (PLS-SXE300, Beijing Trusttech Technology Co., Ltd, China) with a UV cut-off filter (>420 nm) was used as the light source. Photocatalytic reaction temperature was maintained by thermostatic circulating water at around 35 °C. Hydrogen gas was detected with a gas chromatograph (GC, SP-2100, Beijing Beifen-Ruili Analytical Instrument Co., Ltd, China), which was equipped with a thermal conductivity detector (TCD), TDX-01 column, and with N_2 as carrier gas. In a typical photocatalytic experiment, 50 mg of the prepared CdS nanocrystals was dispersed into 200 mL aqueous solution containing 20 mL of lactic acid (LA) and a certain amount of **Co**. Herein, LA was used as sacrificial agent to scavenge photogenerated holes. Then the sus-

pension was purged with N_2 for 20 min to remove air before light irradiation, and the pH value of the obtained photocatalytic suspension was measured to be 1.66. Control experiments showed that no H_2 evolution was detected without light irradiation. For reference, 1 wt% Pt as photo-deposited on CdS under visible light irradiation for 30 min and then used for photocatalytic hydrogen evolution experiment. For the recycling test of CdS/**Co**/LA, the photocatalytic reaction was continued for 4 runs (60 min each run). Typically, before each run, when it ceased, the system was re-added with 0.04 mmol of **Co** directly and some lactic acid to keep pH 1.66, and then purged with N_2 for 20 min to remove air before light irradiation.

The turnover number (TON) for H_2 evolution was calculated according to Eq. (1):

$$\mathrm{TON} = \frac{\text{Number of product molecules}}{\text{Number of catalyst molecules}} = \frac{\text{Number of evolved } H_2 \text{ molecules}}{\text{Number of catalyst molecules}} \quad (1)$$

2.6. Adsorption measurement

The adsorption amount of **Co** onto CdS was determined by the following relation [34]:

$$C_s = \frac{(C_0 - C_e) \times V_s}{m} \quad (2)$$

where C_s is the amount of **Co** adsorbed (mg/g), C_o is the original concentration of **Co** (mg/L), C_e is the equilibrium concentration of **Co** (mg/L), V_s is the solution volume (L), and m is the mass of CdS (g). The concentration of **Co** was determined by UV–vis absorbance according to Bouguer–Lambert–Beer law.

Adsorption data was fitted to the Freundlich model:

$$C_s = K_f C_e^{1/n} \quad (3)$$

or the logarithmic form:

$$\log C_s = \log K_f + \left(1/n\right) \log C_e \quad (4)$$

where K_f represents the Freundlich adsorption coefficient and gives an estimate of the adsorptive capacity, and (1/n) describes the isotherm curvature and gives an estimate of the adsorptive intensity.

2.7. Electrochemical studies

All the electrochemical measurements including, Cyclic voltammetry (CV), Linear sweep voltammograms (LSV) and Mott–Schottky (M–S) measurements were carried out on a potentiostat (273A, Princeton Applied Research Company, USA) in a three-electrode cell system. CV measurements were carried out in the 0.5 M Na_2SO_4 aqueous solution as electrolyte, which was purged using N_2 for 10 min before CV measurements, with glassy carbon as working electrode, a platinum wire as counter electrode and an Ag/AgCl electrode (saturated KCl, named Ag/AgCl) as reference electrode, respectively. LSV and M–S measurements were performed under dark in an aqueous solution of 10 vol% lactic acid (LA) as the electrolyte purged with N_2 for 10 min. The as-prepared films, a large area platinum plate and an Ag/AgCl electrode were employed as working electrode, counter electrode and reference electrode, respectively.

3. Results and discussion

3.1. Interaction between CdS and **Co** coenzyme

In this study, cubic CdS nanocrystals ($E_g \sim 2.43$ eV) with average crystallite size of 4.7 nm (Fig. S1a–c and Table S1 in Supplementary Information, SI) were prepared as photosensitizer by a simple solvothermal method. The **Co** coenzyme was synthesized according to the literature [33]. The element composition in **Co** coenzyme was identified by elemental analyzer to detect the element contents of C, H and O and X-ray fluorescence spectrum (XRF) to detect the element content of Co. The detected element contents in **Co** coenzyme (Co, 13.5%; C, 23.3%; H, 3.7%; N, 13.6%) are very close to the calculated element contents (Co, 14.0%; C, 22.8%; H, 3.8%; N, 13.3%) [33]. Then **Co** coenzyme was confirmed again by UV–vis spectra (Fig. S1d) with optical absorption profile in full agreement with the reported results [33,35], and ESI–MS with a base peak at 408.0210 corresponding to the $[Co(dmgBF_2)_2{\cdot}Na]^+$ ion (Fig. S2).

In order to explore the binding of **Co** onto the CdS nanocrystals, a certain amount of CdS with a specific surface area of 66.8 $m^2\ g^{-1}$ (Table S1) was added to a dilute aqueous solution of **Co**. As shown in Fig. 1a, the data profile of **Co** adsorbed onto CdS nanocrystals fits well with the Freundlich adsorption equation, with a calculated adsorption coefficient of 1.13×10^{-2}. Photoluminescence (PL) spectra were further used to investigate the electron transfer process in the system. As shown in Fig. 1b, CdS exhibits a broad emission centered at 545 nm, which is attributed to the irradiative band-transition recombination of photogenerated electrons and holes [36]. When **Co** was added, the band-transition emission of CdS was quenched dramatically and slightly redshifted from 545 nm to 550 nm, which is likely due to the close interaction between **Co** and CdS [37–39], resulting in efficient electron transfer from CdS to the adsorbed **Co**. Such quenching in PL emission could then confirm the reduced charge recombination in CdS nanocrystals in the presence of the **Co** catalyst in aqueous solution, as referred by the PL quenching of ZnO by $[Fe_2S_2]$ reported by Li and co-workers [40]. To further illustrate the essential role of **Co** in the electron transfer behavior of CdS, photocurrent characterizations were carried out [41,42]. As shown in Fig. S3, the photocurrent of CdS was greatly enhanced when coupled with **Co**, indicating the promoted electron transfer and reduced charge recombination of CdS by **Co** adsorption, which is in good agreement with the PL results.

3.2. Photocatalytic hydrogen production

The photocatalytic H_2 evolution activity of the hybrid CdS/**Co**/LA system was investigated under visible light irradiation ($\lambda > 420$ nm), depending on the concentrations of **Co** and CdS in aqueous solutions. As shown in Fig. 2a, no H_2 is produced when either CdS or LA is absent in the hybrid system, suggesting the indispensability of CdS as the light harvester and LA as the hole scavenger for the half reaction of H_2 evolution [40]. Without molecular **Co** coenzyme, CdS alone shows a very low photocatalytic activity, with H_2 evolution rate of 0.13 μmol/min in the initial 30 min (Fig. 2a). In comparison, the CdS/**Co**/LA hybrid system shows a huge increase of 4000% in the photocatalytic H_2 evolution rate, reaching 5.4 μmol/min in the initial 30 min, which is even 700% as high as that of the CdS/Pt/LA system (0.75 μmol/min). This remarkable enhancement in photocatalytic activity implies that **Co** coenzyme is a highly effective cocatalyst (even active than Pt), promoting electron transfer from CdS to aqueous solution for proton reduction. The detailed mechanism will be discussed in the following sections. Although the photocatalytic H_2 evolution almost ceases after visible irradiation for 60 mins, the photocatalytic stability of this CdS/**Co**/LA hybrid system is greatly improved, as compared to the reported organic photocatalytic system '**P1-Co1**' containing **Co** as H_2 evolution catalyst, which exhibits a very short lifetime of only 6 mins with the same **Co** concentration (0.2 mmol/L) [29]. Although relatively low, the TON for the present AP system (see Eq. (1)), calculated to be 6.3 in 1 h, is still comparable to the previous results on molecular homogeneous systems of '**P1-Co1**' (TON = 2 in 6 min) [29] and 'RB-**Co**' system (TON = 21 in 5 h) [30].

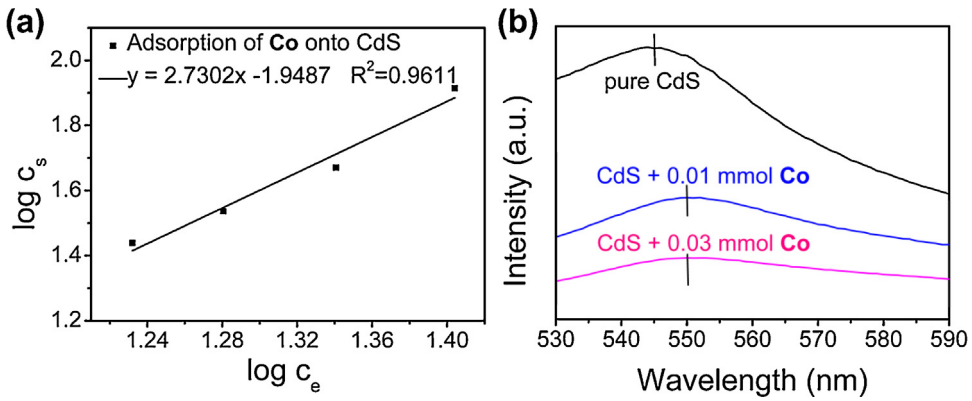

Fig. 1. (a) Model fit of adsorption isotherm of **Co** onto CdS in aqueous solution and (b) PL emission spectra of the CdS suspension (20 mg of CdS in 100 mL of water) with and without **Co**, excited at 325 nm.

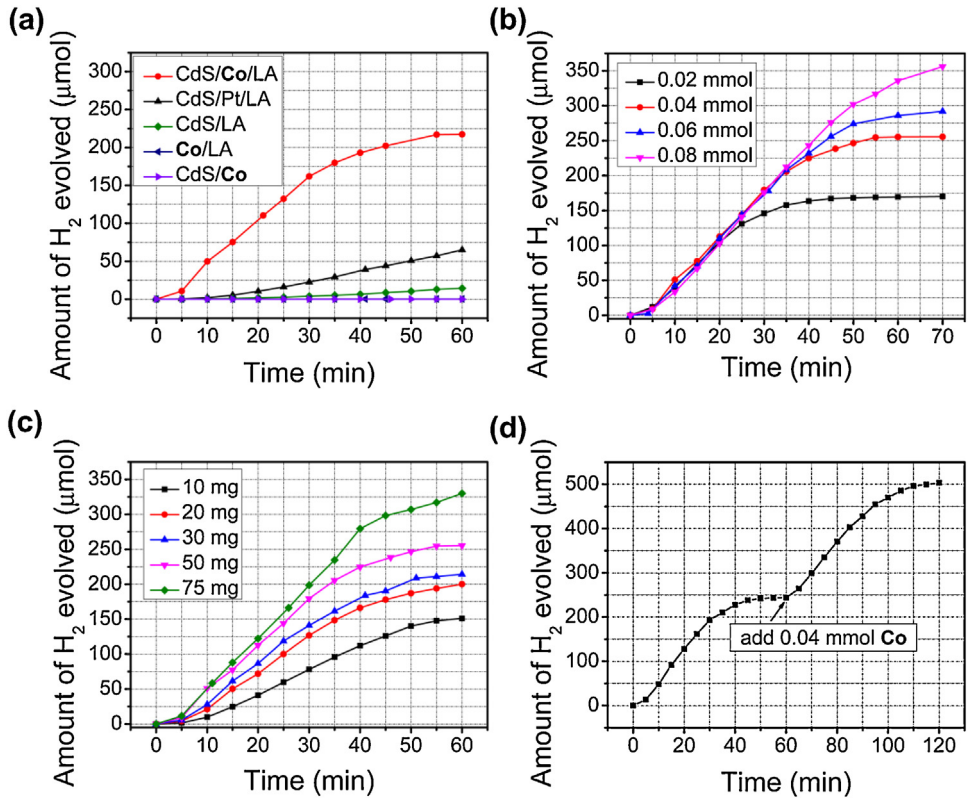

Fig. 2. (a) Time courses of photocatalytic H_2 evolution in different systems, (b) time courses of photocatalytic H_2 evolution in the CdS/**Co**/LA system with different amounts of **Co** and a fixed amount of CdS (50 mg), (c) time courses of photocatalytic H_2 evolution over CdS/**Co**/LA system with different amounts of CdS and a fixed amount of **Co** (0.04 mmol) and (d) time courses of photocatalytic H_2 evolution over CdS/**Co**/LA system with 50 mg of CdS and 0.04 mmol of **Co**, and re-adding of **Co** (0.04 mmol) to the system after irradiation for 60 min. Conditions: 200 mL of 10 vol% LA aqueous solution under visible light irradiation (300 W Xe lamp, λ > 420 nm).

To determine whether the photocatalytic inactivation stems from the decomposition of molecular **Co** catalyst or photocorrosion of CdS, the photocatalytic H_2 evolution activities depending on the amounts of **Co** and CdS were investigated in detail. One can easily find that with the increasing amounts of **Co**, the photocatalytic systems exhibit significantly prolonged lifetime but very similar initial photocatalytic activity (Fig. 2b). The gradual decomposition of **Co** adsorbed on the surface of CdS nanocrystals during the photocatalytic process might be then responsible for the unsatisfying photocatalytic H_2 evolution stability. Note that 50 mg of CdS nanocrystals can only adsorb 22.9 μmol of **Co** in 200 mL of aqueous solution as determined from the Freundlich adsorption equation in Fig. 1a. Given the excessive amounts of **Co** used in Fig. 2b, the saturated adsorption of **Co** onto CdS results in the similar initial photocatalytic activity. In comparison, the increase in the amounts of CdS as photosensitizer does not obviously prolong the lifetime of photocatalytic H_2 evolution (Fig. 2c), implying that the inactivation of this hybrid system is not related to CdS; while the initial photocatalytic activity is greatly improved with increasing amounts of CdS, due to the increasing amounts of **Co** adsorbed on CdS responsible for more efficient H_2 evolution in the initial period (Figs. 2c and S4a). Upon addition of 0.04 mmol of **Co** into the already inactive system (after 60 min reaction), as shown in Fig. 2d, the photocatalytic activity for H_2 evolution could be recovered sufficiently to be comparable to the initial activity, which was further confirmed by the recycling test of the CdS/**Co**/LA system for photocatalytic H_2 evolution as shown in Fig. S5. However, the re-adding of CdS cannot re-activate the photocatalytic H_2 evolution reaction

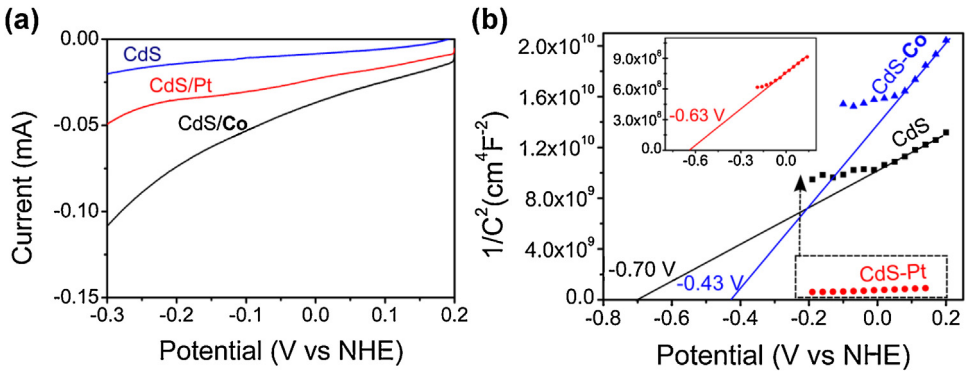

Fig. 3. (a) Linear sweep voltammograms (LSV) and (b) Mott–Schottky (M–S) plots of CdS, CdS/Pt and CdS/**Co** films in 10 vol% LA aqueous solution. Conditions: the prepared films were used as working electrodes and Pt as counter electrodes, before electrochemical measurement the 10 vol% LA aqueous solution as electrolyte was degassed by N_2 for 15 min, scan rate: 100 mV/s.

(not shown). Based on the photocatalytic results above, it could be deduced that the cease of H_2 evolution for the CdS/**Co**/LA system should be caused by the decomposition of **Co** coenzyme with photocatalytic reaction proceeding.

3.3. *Why **Co** coenzyme is more active than Pt: electrochemical investigation*

Although the **Co** coenzyme will be deactivated in 60 min for photocatalytic H_2 generation in the CdS/**Co**/LA system, it is much more stable than the reported lifetime of only 6 min for **Co** in a homogenous molecular AP system photocatalytic H_2 evolution [29]. Moreover, as evidenced in Fig. 2a, **Co** coenzyme is much more effective to catalyze H_2 generation than Pt, with the CdS/**Co**/LA system outperforming the CdS/Pt/LA system in initial H_2 evolution rate as much as 7 times. Thus, it is of great necessity to reveal the crucial role of **Co** coenzyme in the hybrid CdS/**Co**/LA photocatalytic system for H_2 generation. The powdered catalysts are generally used to fabricate film electrodes, in order to get an insight into the electrochemical properties of powder samples [43–45]. Herein, CdS, CdS/Pt and CdS/**Co** films were fabricated and compared as cathodes to reveal the catalysis effect of **Co** for electrocatalytic H_2 generation through electrochemical investigation into the CdS/electrolyte interface.

The linear sweep voltammograms (LSV) for H_2 evolution reaction (HER) of the CdS, CdS/Pt and CdS/**Co** films were tested in 10 vol% LA aqueous solution at sweep rate of 100 mV/s, as shown in Fig. 3a. It is reasonable that the CdS/Pt film shows higher current and anodic shift in onset potential for HER when compared to the CdS film, as noble metal Pt always acts as the highly effective HER catalyst for electrocatalytic and photocatalytic water splitting [46]. Surprisingly, the CdS/**Co** film exhibits even much higher current and more anodic onset potential for HER than the CdS/Pt film, implying that **Co** could act as a more effective HER catalyst than Pt. Note that **Co** coenzyme will not be reduced at the potential of 0.2 V to −0.3 V vs. NHE (the reduction potential of **Co** is about −0.45 V vs. NHE) [47]. This more anodic shift in onset potential and higher current should be then attributed to the **Co** coenzyme adsorbed onto CdS nanocrystals catalyzing HER, leading to the higher initial H_2 evolution rate relative to CdS/Pt (Fig. 2a).

Mott–Schottky (M–S) analysis was conducted for the CdS, CdS/Pt and CdS/**Co** films, to investigate the effects of **Co** coenzyme on the electrochemical and electronic properties of CdS nanocrystals as photocatalyst for H_2 evolution. It has been conceptually well-established in semiconductor physics that when semiconductor and solution are in contact, charges in semiconductor will transfer from the bulk phase to surface, due to the difference between the Fermi level (E_f) of semiconductor and the chemical potential of solution. Then the space charge region [48,49] near the semiconductor surface will be created, which can be described by band bending; and the energy bands always bend upward at the semiconductor/electrolyte interface for n-type semiconductor in aqueous solution, as shown in Scheme 1, which will hinder the charge (electron) transfer to the aqueous solution and form an energy barrier for the following proton reduction (i.e., electrocatalytic or photocatalytic H_2 generation). When CdS and Pt are brought to a typical Schottky contact, the electrons in CdS will tend to flow to Pt due to the lower E_f of Pt than CdS, resulting in positive shift in flat band potential (E_{fb}) of CdS, which has been evidenced in Fig. 3b that a 70 mV positive shift in E_{fb} happens to CdS/Pt relative to bare CdS. Thus, the band bending of CdS will be weakened and then the energy barrier for H_2 generation will be decreased. When compared to CdS/Pt, as shown in Fig. 3b and Scheme 1, a much bigger positive shift of 270 mV in E_{fb}, corresponding to an increase of 270 meV in CdS work function, is observed for CdS/**Co**, indicating the much more decrease in band bending of CdS. Hence, electron transfer from CdS to **Co** coenzyme is more efficient than from CdS to Pt, due to the close interaction of CdS and **Co** (as evidenced by PL results), and energy barrier for HER at semiconductor/electrolyte interface is much lower. All the electrochemical observations mean that **Co** coenzyme could be a more effective HER catalyst than Pt. Based on the discussion of LSV and M–S above, it can be concluded that the photogenerated electron transfer from CdS to **Co** is more efficient than from CdS to Pt, due to the larger positive shift of E_{fb} and then the much more decrease in band bend-

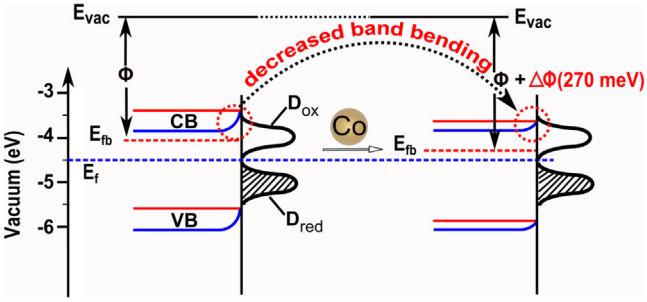

Scheme 1. The proposed band structure at the CdS/electrolyte interface without or with **Co** coenzyme in aqueous solution. E_{fb}: flat-band potential, E_f: Femi level, Φ: work function, E_{vac}: vacuum energy, D_{ox} and D_{red}: density of unoccupied states and occupied states of the redox electrolyte system, respectively. Blue solid lines represent the CB (conduction band) or VB (valence band) in the M–S measurement. Red solid lines represent the CB or VB counterbalanced in the M–S measurement. (For interpretation of the references to colour in this figure legend, the reader is referred to the web version of this article.)

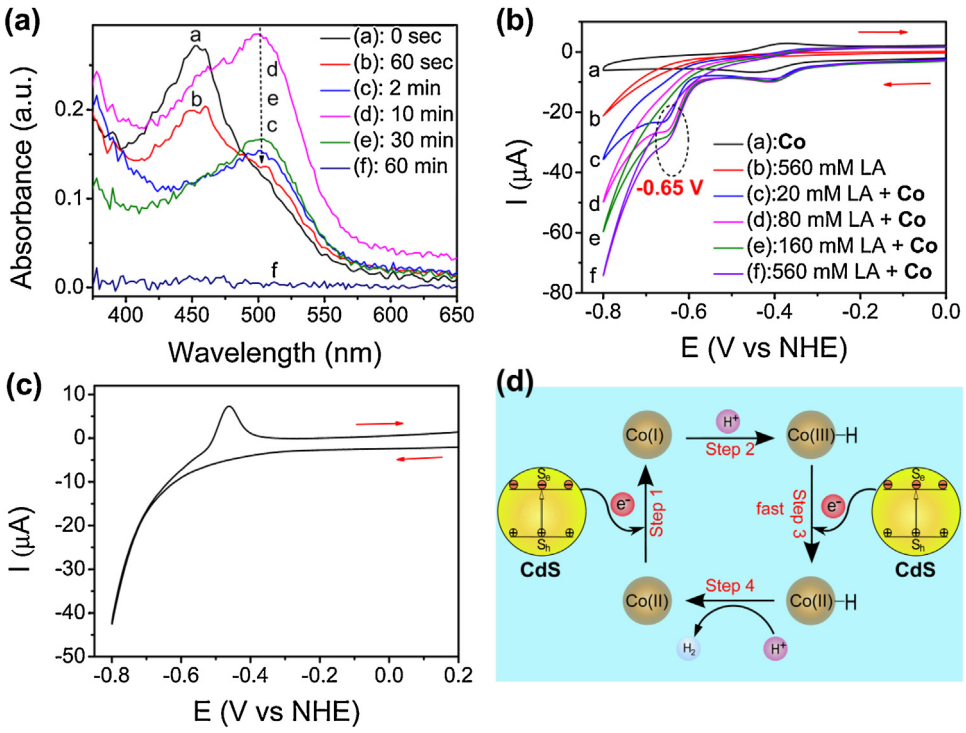

Fig. 4. (a) UV–vis spectra of the solutions in CdS/**Co**/LA H_2 evolution system under visible light irradiation for different times, (b) Cyclic voltammetry (CV) measurement of the aqueous solution containing 0.15 mM **Co** without or with different amounts of LA, (c) CV measurement of the supernatant obtained by centrifuging the CdS/**Co**/LA suspension after 15 min photocatalytic reaction, and (d) the catalysis mechanism of **Co** for H_2 evolution. Conditions of UV–vis tests: CdS (50 mg), **Co**(0.04 mmol), 200 mL of 10 vol% aqueous solution of sacrificial reagents, Xe lamp (300 W, λ > 420 nm); Conditions of CV tests: degassed aqueous solution with 0.5 M Na_2SO_4 as supporting electrolyte, scan rate 100 mV/s, glassy carbon as working electrodes and Pt as counter electrodes.

ing, leading to the smaller energy barrier or overpotential for HER at semiconductor/electrolyte interface.

3.4. *Catalysis mechanism of **Co** coenzyme for photocatalytic hydrogen evolution*

To investigate the catalysis mechanism of **Co** coenzyme in the photocatalytic process, the change in optical properties of the CdS/**Co**/LA system were monitored by UV–vis spectra during photocatalytic H_2 evolution. In the typical measurement, the suspensions of the hybrid CdS/**Co**/LA photocatalytic systems were sampled at intervals using syringe pumps, followed by high speed centrifugation to get supernatant for UV–vis test. As shown in Figs. 4 a and S6a, the characteristic absorption peak of **Co** at ca. 456 nm decreases rapidly in the initial 2 min under visible irradiation; meanwhile a new absorption peak at ca. 500 nm emerges, possibly indicating a new **Co** species generated from the original **Co** coenzyme during photocatalytic H_2 evolution. Apparently, the increasing absorbance for the characteristic peak of **Co** at ca. 456 nm from 2 min to 10 min in Fig. S6b is ascribed to emergence of the peak at ca. 500 nm. Moreover, the absorption intensity at ca. 500 nm, indicative of the amount of this new '**Co** species', gradually increases in the initial 10 min and then decreases with photocatalytic reaction proceeding to 60 min. One can find that this new absorption peak completely disappears after 60 min, exactly at the same time when H_2 evolution ceases (Fig. 2a). Thus, it is assumed that in the CdS/**Co**/LA hybrid system this intermediate '**Co** species' with characteristic absorption peak at ca. 500 nm might be catalytically active for H_2 evolution. The possible functional mechanism of the catalytically active '**Co** species' intermediate in the hybrid CdS/**Co**/LA system will be investigated in the following sections.

In an AP photocatalytic system, electrochemical characterization is powerful to provide deep insight into the catalytic mechanisms. As shown in Fig. 4b, the cyclic voltammetry (CV) of **Co** coenzyme shows a reversible one-electron wave at −0.42 V vs. NHE, which could be assigned to the **Co**(II)/**Co**(I) redox couple (−0.42 V vs. NHE) and is in good agreement with the literatures [47,50]. Adding some LA into the **Co** aqueous solution gives rise to the higher current density of the **Co**(II)/**Co**(I) response, meaning a faster reduction of **Co**(II) coenzyme with LA acting as electron donor. Given that the conduction band potential of CdS nanocrystals (−0.9 V vs. NHE) [51] is more negative than the reduction potential of **Co**(II) to **Co**(I) (−0.42 V vs. NHE), it is thermodynamically favorable for the photogenerated electrons in the conduction band of CdS nanocrystals to transfer to **Co**(II) and produce electronegative **Co**(I) species. The **Co**(I) species are then supposed to turn to **Co**(III)-H species via protonation, due to the lower free energy of **Co**(III)-H relative to **Co**(I) [52] and the high pKa (13.3) [47] of the **Co**(III)-H/**Co**(I) in the solution with initial pH = 1.66 (the most suitable pH for H_2 evolution as shown in Fig. S7) for the present CdS/**Co**/LA system. Moreover, as shown in Fig. 4b, a new irreversible cathodic wave is triggered near −0.65 V vs. NHE upon adding LA. As discussed in previous study [47], this new cathodic wave should be related to the reduction of **Co**(III)-H, and the increasing height of this wave means that the **Co**(III)-H reduction reaction is accelerating with the increasing amounts of LA in aqueous solution. This emerged cathodic wave, however, cannot be observed during the supplementary CV measurement of the supernatant obtained by centrifuging the CdS/**Co**/LA suspension after 15 min photocatalytic reaction (Fig. 4c). It could be then deduced that the **Co**(III)-H species can hardly exist as the stable immediate during photocatalytic H_2 generation under visible light, but tend to get another photogenerated electron from CdS to form **Co**(II)-H species very quickly, given the more negative conduction band potential of CdS (−0.9 V vs. NHE) than the redox potential of **Co**(III)-H/**Co**(II)-H (−0.65 V vs. NHE). Thus, different from the intermediate **Co**(I) species with absorptions at ca. 610 nm

reported in other studies [30,53], the essential intermediate '**Co** species' detected in UV–vis spectra should be **Co**(II)-H, which acts as the catalytically active intermediate reacting with one proton or another **Co**(II)-H species to generate H_2 in the hybrid CdS/**Co**/LA photocatalytic system under visible light irradiation. Honestly, it is difficult to directly confirm the molecular structure of the intermediate '**Co** species' catalytically active for H_2 generation; however, it is still reasonable to deduce **Co**(II)-H as the active intermediate based on the charge transfer processes and physicochemical properties of the **Co**-based species as discussed above.

One may note that the initial rate of CdS/**Co**/LA systems with different amounts of **Co** are similar (Fig. 2b), due to the excessive **Co** in aqueous solution giving rise to the saturated adsorption of **Co** onto CdS nanocrystals (50 mg) in the initial period of photocatalytic reaction. Such saturated adsorption makes it impossible to compare the initial H_2 evolution rates depending on the amounts of **Co** as HER catalyst adsorbed onto CdS nanocrystals. Thus, to further determine whether the **Co**(II)-H species undergo protonation to generate H_2 (monometallic mechanism) [23], or reacted with another **Co**(II)-H molecule to evolve H_2 (bimetallic mechanism) [23], the initial H_2 evolution rates depending on the amounts of **Co** adsorbed onto CdS nanocrystals by diluting **Co** concentrations in aqueous solutions, were investigated in detail. As shown in Fig. S4b, the initial H_2 evolution rates perform linear dependence on the concentrations of **Co** in the CdS/**Co**/LA photocatalytic systems, indicative of the monometallic mechanism in the present study, which is very common in photocatalytic and electrocatalytic H_2 production [54,55] Therefore, the possible charge transfer and catalysis processes in the CdS/**Co**/LA system for photocatalytic H_2 generation could be proposed as an ECEC mechanism in Fig. 4d. Typically, under visible light irradiation, **Co** coenzyme is initially reduced by the photogenerated electrons in the conduction band of CdS nanocrystals to be **Co**(I) (step 1), which is then protonated to be **Co**(III)-H (step 2) and quickly reduced again by photogenerated electrons to be **Co**(II)-H (step 3); the generated **Co**(II)-H intermediate actively catalyzes H_2 evolution via protonation (step 4). Through the ECEC process, the photogenerated electrons from CdS can be efficiently utilized by **Co** for H_2 generation.

4. Conclusions

In summary, we present a noble-metal-free hybrid system of artificial photosynthesis for H_2 generation from a fully aqueous solution containing CdS nanocrystals as the light harvester, $Co(dmgBF_2)_2(H_2O)_2$ (**Co**) coenzyme as the redox catalyst and lactic acid (LA) as the sacrificial agent. The initial H_2 generation rate of this typical CdS/**Co**/LA system is 40 and 7 times as high as that of CdS/LA and CdS/Pt/LA, respectively. The excellent photocatalytic performance of CdS/**Co**/LA system should be attributed to the efficient electron transfer from CdS to **Co**, leading to promoted charge separation and reduced charge recombination, as well as the positively shifted Fermi level of CdS, decreasing the overpotential for catalyzing H_2 generation at the CdS/electrolyte interface. It was supposed that the electron-coupling-electron-coupling (ECEC) process, involving with the reduction of **Co** coenzyme followed by protonation and then reduction again to produce the **Co**(II)-H intermediate active for catalyzing H_2 evolution, was responsible for the photocatalytic H_2 evolution in the CdS/**Co**/LA hybrid system. The **Co**-promoted charge transfer and the **Co**-catalyzed proton reduction reaction together boosted the photocatalytic activity of the CdS/**Co**/LA system for artificial photosynthesis for H_2 generation. This study presents a systematic investigation into the mechanism of hybrid artificial photosynthesis system for H_2 generation, providing some referable guidelines for surface engineering of semiconductor nanocrystals with metal organic molecules as catalysts for solar H_2 conversion from the viewpoint of surface/interface chemistry and physics.

Acknowledgements

The authors gratefully acknowledge the financial support of the National Natural Science Foundation of China (51323011, 51236007), the Program for New Century Excellent Talents in University (NCET-13-0455), the Natural Science Foundation of Shaanxi Province (2014KW07-02), the Natural Science Foundation of Jiangsu Province (BK 20141212) and the Nano Research Program of Suzhou City (ZXG201442, ZXG 2013003). S. Shen is supported by the Foundation for the Author of National Excellent Doctoral Dissertation of P. R. China (201335), the National Program for Support of Top-notch Young Professionals, and the "Fundamental Research Funds for the Central Universities".

Appendix A. Supplementary data

Supplementary data associated with this article can be found, in the online version, at http://dx.doi.org/10.1016/j.apcatb.2016.06.029.

References

[1] X. Chen, S. Shen, L. Guo, S.S. Mao, Chem. Rev. 110 (2010) 6503–6570.
[2] T. Hisatomi, J. Kubota, K. Domen, Chem. Soc. Rev. 43 (2014) 7520–7535.
[3] S.S. Mao, S. Shen, Nat. Photonics 7 (2013) 944–946.
[4] L. Hammarström, Acc. Chem. Res. 42 (2009) 1859–1860.
[5] S. Wang, W. Yao, J. Lin, Z. Ding, X. Wang, Angew. Chem. Int. Ed. 53 (2014) 1034–1038.
[6] S. Wang, X. Wang, Small 11 (2015) 3097–3112.
[7] S. Wang, W. Yao, J. Lin, Z. Ding, X. Wang, Angew. Chem. Int. Ed. 53 (2014) 1034–1038.
[8] F. Wen, C. Li, Acc. Chem. Res. 46 (2013) 2355–2364.
[9] M. Wang, K. Han, S. Zhang, L. Sun, Coordin. Chem. Rev. 287 (2015) 1–14.
[10] A. Reynal, F. Lakadamyali, M.A. Gross, E. Reisner, J.R. Durrant, Energy Environ. Sci. 6 (2013) 3291–3300.
[11] M.A. Gross, A. Reynal, J.R. Durrant, E. Reisner, J. Am. Chem. Soc. 136 (2014) 356–366.
[12] H. Tseng, M.B. Wilker, N.H. Damrauer, G. Dukovic, J. Am. Chem. Soc. 135 (2013) 3383–3386.
[13] K. Han, M. Wang, S. Zhang, S. Wu, Y. Yang, L. Sun, Chem. Commun. 51 (2015) 7008–7011.
[14] M. Matsumura, S. Furukawa, Y. Saho, H. TsubOmura, J. Phys. Chem. 89 (1985) 1327–1329.
[15] K. Zhang, L. Guo, Catal. Sci. Technol. 3 (2013) 1672–1690.
[16] D. Jing, L. Guo, J. Phys. Chem. B 110 (2006) 11139–11145.
[17] Q. Li, B. Guo, J. Yu, J. Ran, B. Zhang, H. Yan, J.R. Gong, J. Am. Chem. Soc. 133 (2011) 10878–10884.
[18] K. Wu, Z. Chen, H. Lv, H. Zhu, C.L. Hill, T. Lian, J. Am. Chem. Soc. 136 (2014) 7708–7716.
[19] B.H. Solis, S. Hammes-Schiffer, Inorg. Chem. 53 (2014) 6427–6443.
[20] E. Anxolabéhère-Mallart, C. Costentin, M. Fournier, M. Robert, J. Phys. Chem. C 118 (2014) 13377–13381.
[21] N.M. Muresan, J. Willkomm, D. Mersch, Y. Vaynzof, E. Reisner, Angew. Chem. Int. Ed. 51 (2012) 12749–12753.
[22] J. Huang, K.L. Mulfort, P. Du, L.X. Chen, J. Am. Chem. Soc. 134 (2012) 16472–16475.
[23] H. Yan, J. Yang, G. Ma, G. Wu, X. Zong, Z. Lei, J. Shi, C. Li, J. Catal. 266 (2009) 165–168.
[24] T. Lazarides, T. McCormick, P. Du, G. Luo, B. Lindley, R. Eisenberg, J. Am. Chem. Soc. 131 (2009) 9192–9194.
[25] T.M. McCormick, B.D. Calitree, A. Orchard, N.D. Kraut, F.V. Bright, M.R. Detty, R. Eisenberg, J. Am. Chem. Soc. 132 (2010) 15480–15483.
[26] T.M. McCormick, Z. Han, D.J. Weinberg, W.W. Brennessel, P.L. Holland, R. Eisenberg, Inorg. Chem. 50 (2011) 10660–10666.
[27] R.P. Sabatini, B. Lindley, T.M. McCormick, T. Lazarides, W.W. Brennessel, D.W. McCamant, R. Eisenberg, J. Phys. Chem. B 120 (2016) 527–534.
[28] Z.Y. Wang, H. Rao, M.F. Deng, Y.T. Fan, H.W. Hou, Phys. Chem. Chem. Phys. 15 (2013) 16665–16671.
[29] L. Li, L. Duan, F. Wen, C. Li, M. Wang, A. Hagfeldt, L. Sun, Chem. Commun. 48 (2012) 988–990.
[30] P. Zhang, M. Wang, J. Dong, X. Li, F. Wang, L. Wu, L. Sun, J. Phy. Chem. C 114 (2010) 15868–15874.
[31] Z. Han, R. Eisenberg, Acc. Chem. Res. 47 (2014) 2537–2544.
[32] A. Cao, Z. Liu, S. Chu, M. Wu, Z. Ye, Z. Cai, Y. Chang, S. Wang, Q. Gong, Y. Liu, Adv. Mater. 22 (2010) 103–106.

[33] A. Bakac, J.H. Espenson, J. Am. Chem. Soc. 106 (1984) 5197–5202.
[34] Y. Wan, Y. Bao, Q. Zhou, Chemosphere 80 (2010) 807–812.
[35] G.W. Wangila, R.B. Jordan, Inorg. Chim. Acta 358 (2005) 2804–2812.
[36] J. Liu, X. Pu, D. Zhang, H.J. Seo, K. Du, P. Cai, Mater. Res. Bull. 57 (2014) 29–34.
[37] H. Zhang, X. Lv, Y. Li, Y. Wang, J. Li, ACS Nano 4 (2010) 380–386.
[38] C. Kong, S. Min, G. Lu, ACS Catal. 4 (2014) 2763–2769.
[39] N. Zhang, J. Shi, F. Niu, J. Wang, L. Guo, Phys. Chem. Chem. Phys. 17 (2015) 21397–21400.
[40] F. Wen, X. Wang, L. Huang, G. Ma, J. Yang, C. Li, ChemSusChem 5 (2012) 849–853.
[41] S. Wang, X. Wang, Appl. Catal. B: Environ. 162 (2015) 494–500.
[42] S. Wang, J. Lin, X. Wang, Phys. Chem. Chem. Phys. 16 (2014) 14656–14660.
[43] J. Bandara, C.P.K. Udawatta, C.S.K. Rajapakse, Photochem. Photobiol. Sci. 4 (2005) 857–861.
[44] L. Liao, Q. Zhang, Z. Su, Z. Zhao, Y. Wang, Y. Li, X. Lu, D. Wei, G. Feng, Q. Yu, X. Cai, J. Zhao, Z. Ren, H. Fang, F. Robles-Hernandez, S. Baldelli, J. Bao, Nat. Nanotechnol. 9 (2013) 69–73.
[45] S. Yang, Y. Gong, J. Zhang, L. Zhan, L. Ma, Z. Fang, R. Vajtai, X. Wang, P.M. Ajayan, Adv. Mater. 25 (2013) 2452–2456.
[46] Y. Li, G. Lu, S. Li, Appl. Catal. A: Gen. 214 (2001) 179–185.
[47] C. Baffert, V. Artero, M. Fontecave, Inorg. Chem. 46 (2007) 1817–1824.
[48] A.J. Nozik, R. Memming, J. Phys. Chem. 100 (1996) 13061–13078.
[49] Z. Zhang, J.T. Yates, Chem. Rev. 112 (2012) 5520–5551.
[50] P. Connolly, E. James, Inorg. Chem. 25 (1986) 2684–2688.
[51] K. Kalyanasundaram, E. Borgarello, M. Grätzel, Helv. Chim. Acta 64 (1981) 362–366.
[52] B.H. Solis, S. Hammes-Schiffer, Inorg. Chem. 53 (2014) 6427–6443.
[53] J. Hawecher, J.M. Lehn, R. Ziessel, Nouv. J. Chim. 7 (1983) 271–277.
[54] A. Das, Z. Han, W.W. Brennessel, P.L. Holland, R. Eisenberg, ACS Catal. 5 (2015) 1397–1406.
[55] Z. Han, L. Shen, W.W. Brennessel, P.L. Holland, R. Eisenberg, J. Am. Chem. Soc. 135 (2013) 14659–14669.